

# Soft Landing of Complex Molecules on Surfaces\*

Grant E. Johnson, Qichi Hu, and Julia Laskin

Fundamental Science Directorate, Pacific Northwest National Laboratory, Richland, Washington 99352; email: Grant.Johnson@pnl.gov, Qichi.Hu@pnl.gov, Julia.Laskin@pnl.gov

Annu. Rev. Anal. Chem. 2011. 4:83–104

First published online as a Review in Advance on March 1, 2011

The *Annual Review of Analytical Chemistry* is online at [anchem.annualreviews.org](http://anchem.annualreviews.org)

This article's doi:

10.1146/annurev-anchem-061010-114028

1936-1327/11/0719-0083\$20.00

\*This is a work of the U.S. Government and is not subject to copyright protection in the United States.

## Keywords

mass-selected ion deposition, proteins, peptides, clusters, organometallic complexes

## Abstract

Soft and reactive landing of mass-selected ions onto surfaces has become a topic of substantial interest due to its promising potential for the highly controlled preparation of materials. For example, there are possible applications in the production of peptide and protein microarrays for use in high-throughput screening, protein separation and conformational enrichment of peptides, redox protein characterization, thin-film production, and the preparation of catalysts through deposition of clusters and organometallic complexes. Soft landing overcomes many of the limitations associated with conventional thin-film production techniques and offers unprecedented selectivity and specificity of preparation of deposited species. This review discusses the fundamental aspects of soft and reactive landing of mass-selected ions on surfaces that pertain to applications of these techniques in biomaterials, molecular electronics, catalysis, and interfacial chemistry.

**Electrospray ionization (ESI):** a process in which ionized species in the gas phase are produced from a solution via highly charged fine droplets by means of spraying the solution from a narrow-bore needle tip at atmospheric pressure in the presence of a high electric field (1,000 to 10,000 V potential)

**Laser vaporization:** removal of material from a solid or liquid sample with energy delivered by a short laser pulse to form ionized gas-phase species and particles

**Magnetron sputtering:** formation of gas-phase ions and particles through the removal of atomized material from a solid via energetic bombardment of its surface layers by ions

**Molecular layer deposition (MLD):** a process in which molecules are stacked on substrates one by one in order of preference in vacuum

**Cluster:** a small group of atoms or molecules

**Secondary structure:** the conformation at a local region of a polypeptide

## 1. INTRODUCTION

Mass spectrometry is a versatile technique for the identification and structural characterization of large molecules. The advent of soft ionization techniques such as electrospray ionization (ESI) (1–2) has enabled the ionization of a wide variety of complex molecules without significant fragmentation, and nonthermal ion sources such as laser vaporization (3–4) and magnetron sputtering (5–6) have provided access to materials that currently cannot be produced through conventional techniques. Most mass spectrometry studies rely on ionization of a molecule of interest or of a complex mixture followed by mass analysis. Alternatively, mass spectrometry may be used as a preparatory technique in which mass-selected ions are deposited onto solid supports or into liquid materials (7–18). Preparatory mass spectrometry offers several unique advantages for deposition of complex molecules on substrates, including the ability to generate high-purity uniform films (19–20), unprecedented selectivity and specificity of preparation of deposited species (11, 21–22), the ability to focus and pattern an ion beam (23–24), and flexibility in both ion-formation (1, 3, 25–26) and mass-selection (27–32) processes. This review highlights applications of mass-selected deposition of complex molecules for selective immobilization of biological molecules and catalytically active complexes on substrates.

Deposition of high-purity thin films is widely used in materials science and microfabrication (33). Molecular layer deposition (MLD) that relies on self-limiting surface reactions between polyatomic molecules and surfaces is the method of choice for preparation of ultrathin organic films and mixed organic-inorganic interfaces (34–35). MLD is often preferred over solution-phase approaches because it enables a substantially higher degree of control over the deposition process and hence produces high-quality films (36). Despite its widespread use, MLD suffers from several limitations, which are discussed in a recent review (37). Specifically, because MLD relies on gas-phase deposition of neutral molecules, it is usually limited to thermally stable organic reactants that have sufficient vapor pressure. In addition, the reactivity of molecules with solid supports is often reduced in the absence of solvent. Here, we demonstrate that deposition of hyperthermal ions overcomes these limitations. First, soft ionization techniques can produce ions of thermally labile molecules of low volatility without significant fragmentation, and nonthermal ion sources can generate a variety of homogeneous or heterogeneous clusters that are not amenable to thermal volatilization. Second, ions may be easily accelerated prior to deposition to the kinetic energy that is necessary to overcome the barrier associated with an interfacial reaction.

In this review, we discuss the fundamental aspects of soft landing (SL) and reactive landing (RL) of mass-selected ions on surfaces that pertain to future applications of these techniques in biomaterials, molecular electronics, catalysis, and interfacial chemistry. SL was first described in 1977 by Cooks and coworkers (7) for collisions of small sulfur-containing ions with metal surfaces; intact deposition of mass-selected ions with charge retention was reported by the same group 20 years later (38). Subsequent studies showed that complex ions, including clusters (39–45), organometallic complexes (46–50), peptides (11, 22, 51–57), proteins (9, 11, 23, 58), DNA (59), and viruses (60), may be deposited on substrates as intact species. Furthermore, retention of charge (57), secondary structure (55), and biological activity (23) has been demonstrated for peptides and proteins soft-landed onto surfaces, and deposition of mass-selected clusters (14, 61–63) and organometallics (46–47, 64–68) has provided an alternative approach for the preparation of monodisperse catalyst materials (63).

RL is a process in which ion-surface collision induces interfacial reactions (24, 69–70). Depending on the properties of the projectile and the surface, RL can initiate a variety of reactions. Examples of RL include patterning of  $\text{Si}(\text{CD}_3)_3^+$  ions on OH-terminated self-assembled monolayer (SAM) surfaces (71); controlled modification of polystyrene surfaces by collisions of

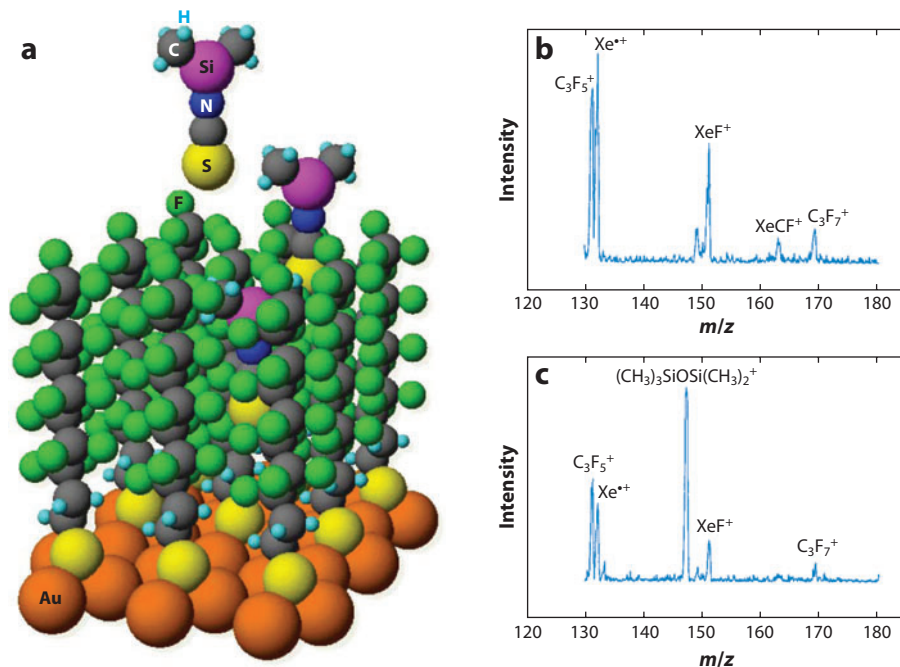


**Figure 1**

(a) Three-dimensional molecular modeling representation of the soft-landing process for  $(\text{CH}_3)_2\text{SiNCS}^+$  projectile ions impinging on a fluorinated self-assembled monolayer (FSAM) surface. (b,c) Mass spectra recorded by 60-eV  $\text{Xe}^+$  sputtering of (b) an FSAM surface and (c) the same surface after treatment for 1 h at a collision energy of 5 eV, with  $(\text{CH}_3)_3\text{SiOSi}(\text{CH}_3)_2^+$  ions ( $m/z$  147), at a total dose corresponding to 7% of a monolayer. Reproduced from Reference 38 with permission. Copyright 2003, American Association for the Advancement of Science.

low-energy  $\text{CF}_3^+$  and  $\text{C}_3\text{F}_5^+$  ions (72–73); pinning of size-selected  $\text{Ag}_{147}^+$  clusters to a graphite surface (74); reactive deposition of mass-selected metal-carbon ( $\text{M}_8\text{C}_{12}^+$ ) clusters on carbon-covered grids, which results in cluster assembly (75); covalent bond formation between  $\text{C}_{58}^+$  clusters deposited onto a graphite surface (76); covalent immobilization of peptides (54, 56) and proteins (58); and many others.

The physical and chemical processes that occur during the interaction of hyperthermal (<100-eV) ions with surfaces, including elastic and inelastic scattering, charge transfer, dissociation, and SL and RL, have been extensively reviewed (10, 55, 77–85). Charge retention has a significant effect on both the structure and the reactivity of deposited complex molecules. Neutralization of projectile ions by electron transfer to or from the surface is a dominant process in collisions of complex ions with metal surfaces (78, 86). The extent of neutralization is substantially reduced when conductive substrates are coated with insulating thin films (84). The deposition of intact polyatomic ions with charge retention was first demonstrated for collisions of  $(\text{CH}_3)_2\text{SiNCS}^+$  ions with fluorinated SAM (FSAM) surfaces (38). **Figure 1a** illustrates an SL experiment in which one ion approaches the surface and two ions are embedded into the layer. Intact polyatomic ions trapped in the FSAM for many days were subsequently released from the matrix by low-energy  $\text{Xe}^+$  sputtering (**Figure 1b,c**). At relatively high collision energies, ion deposition may result in fragmentation of the projectile and trapping of the resulting fragments (87). This deposition regime is known as crash landing. Surprisingly, no crash landing was observed for

**Secondary ion mass spectrometry (SIMS):**

a type of mass spectrometry in which secondary ions are ejected from a sample surface as a result of bombardment by a primary beam of atoms or ions

**Time-of-flight secondary ion mass spectrometry (TOF-SIMS):**

a technique that uses a pulsed primary ion beam to desorb and ionize a species from a sample surface for subsequent mass analysis by time of flight from the surface to a detector

**Fourier transform infrared spectroscopy (FTIR):**

a technique that simultaneously collects infrared spectral information in a wide range of wavelengths

**Amide I:** a vibrational band of peptides and proteins that involves mainly the carbonyl-stretching vibrations of the peptide backbone and is a sensitive marker of peptide secondary structure

deposition of peptide ions on SAM surfaces at the fairly high collision energy of 150 eV, which suggests that the internal excitation was rapidly dissipated by the trapped ions. Similar results were reported for SL of crystal violet on plasma-treated silver substrates and for deposition of proteins onto liquid surfaces (88).

## 2. SOFT LANDING AND REACTIVE LANDING OF BIOMOLECULES

Deposition of peptides and proteins on surfaces is of interest for various biological applications ranging from characterization of molecular recognition events at the amino acid level and identification of biologically active motifs in proteins to the development of novel biosensors and substrates for improved cell adhesion. It is also important for the understanding of interactions between peptides/proteins and surfaces in the absence of solvent (89–94).

The process of immobilizing biomolecules on substrates often utilizes SAM surfaces because of their well-defined structure and biocompatibility and the availability of various terminal functional groups that control the physical and chemical properties of the monolayer (90, 95). Peptides and proteins adsorbed onto SAMs are held either by weak van der Waals forces when the SAM is terminated with nonreactive functional groups (e.g., CH<sub>3</sub> or CF<sub>3</sub>) or by strong electrostatic binding with the COOH-terminated SAM (COOH-SAM) (55). Alternatively, biomolecules may be covalently attached to SAM surfaces terminated with reactive groups [e.g., N-hydroxysuccinimide (NHS), 16-mercaptohexadecanoic acid fluoride, anhydride, etc.], an important prerequisite for the fabrication of protein microarrays and biosensors, the synthesis of biomaterials, and other biotechnology applications (54, 96). Existing approaches for the immobilization of biomolecules onto SAMs are based on solution-phase synthetic strategies and require relatively large quantities of purified material. Alternatively, SL and RL may be utilized for highly specific preparation of biomolecules on substrates, which eliminates the effects of solvent, sample contamination, and analyte agglomeration in solution on the quality of the film.

### 2.1. Deposition of Peptide Ions

Systematic studies of the SL of protonated peptides on surfaces demonstrated that when the FSAM surface is used as a target, a substantial number of ions retain one and two protons (57, 97). In situ secondary ion mass spectrometry (SIMS) experiments indicated that a singly protonated peptide is formed by partial proton loss of a deposited doubly protonated molecule, and complete neutralization occurs mainly at the time of ion-surface collision (97). Partial charge retention was also observed for multiply protonated proteins soft-landed onto FSAM surfaces (9). Comparing the rates of proton loss on different SAM surfaces indicated that the neutralization efficiency increases in the order FSAM < HSAM < COOH-SAM (53).

Covalent immobilization of peptides with RL was studied using arginine-glycine-aspartate (RGD)-containing peptides as model systems (54, 56). Synthetic surfaces containing the RGD motif are commonly used for stimulated cell adhesion. Deposition of a doubly protonated cyclic pentapeptide c(RGDfk) onto an NHS-SAM surface resulted in covalent linking of the peptide through formation of an amide bond between the surface and the amino group of the lysine side chain (**Figure 2a**) (56). The nature of the binding was determined by time-of-flight SIMS (TOF-SIMS) and Fourier transform infrared spectroscopy (FTIR) characterization of the modified NHS-SAM. Local coverage obtained via RL was estimated by comparing the intensities of the amide I band of the peptide immobilized using solution-phase chemistry and RL. Remarkably, similar local coverage of 60% of a monolayer was obtained in comparable reaction times of 4 h for RL and 2 h for reaction in solution, whereas RL required only one-fiftieth as much material

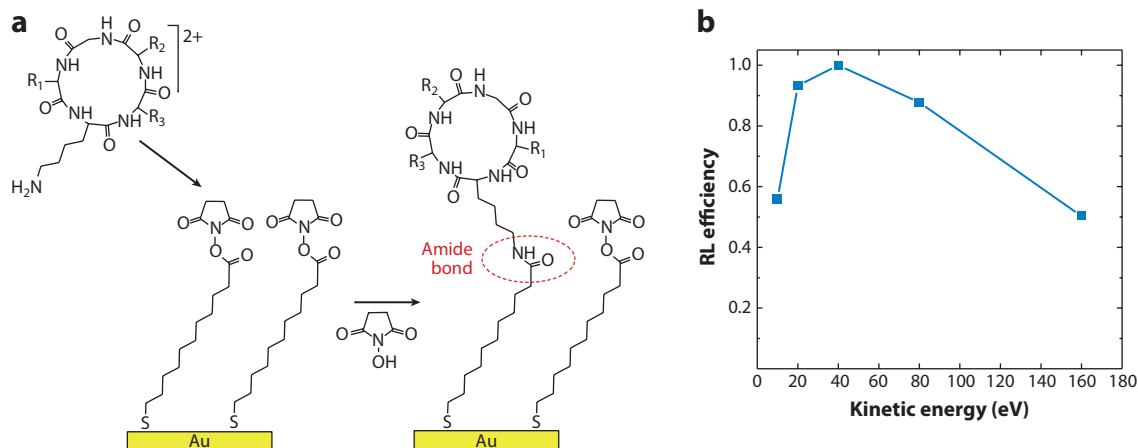


**Figure 2**

(a) Schematic drawing of reactive landing (RL) of the doubly protonated cyclic pentapeptide c(RGDFK) onto an N-hydroxysuccinimide self-assembled monolayer surface. (b) RL efficiency as a function of the kinetic energy of the projectile ion. Reproduced from Reference 54 with permission. Copyright 2008, Royal Society of Chemistry.

(56). In another experiment, the local coverage obtained for RL of a linear GRGDSPK peptide was approximately 15 times higher than the coverage obtained in solution after the same reaction time (54). These findings indicate that surface modification performed with RL is very efficient and requires smaller amounts of material than do traditional approaches.

A subsequent study demonstrated that the reaction takes place during collision between the ion and the surface (54). The reaction yield in these experiments was independent of the charge state of the projectile ion, which indicates that efficient neutralization of peptide ions took place upon collision. In contrast, the kinetic energy of the projectile ion has a strong effect on the RL efficiency. **Figure 2b** shows that RL efficiency increases with collision energy, reaches a maximum at approximately 40 eV, and gradually decreases at higher collision energies because of the competition between RL and scattering of ions off the surface (54). Similar behavior was reported for RL of small organic ions (50, 71, 98) and proteins (58). The increase in RL efficiency with collision energy indicates that the reaction is associated with a substantial barrier that is responsible for the slow reactivity of peptide molecules with an NHS-SAM in solution. Apparently, local heating of the surface during ion-surface collision efficiently promotes the reaction, leading to high yields of RL products. Therefore, the RL approach has a significant advantage, given that heating of the entire substrate in solution to achieve a higher reactive yield may result in melting and degradation of the SAM (99). The RL efficiency was estimated by examining collisions of protonated diaminododecane with NHS-SAM. Almost every collision between this simple projectile ion and the surface results in bond formation (100).

RL of peptides on surfaces enables characterization of their redox properties. For example, Mazzei et al. (101) and Pepi et al. (102) used cyclic voltammetry (CV) to examine the electrochemical properties of microperoxidase 11 (MP-11)—an undecapeptide that contains the active-site microenvironment of cytochrome *c*—deposited on gold surfaces and on multiwalled carbon nanotubes (103). The authors demonstrated that MP-11 deposited on both substrates is stable and retains its native properties and electron-transfer functionality. Detailed analysis of the electron-transfer kinetics, redox potential, and reorganization energy indicated that the soft-landed MP-11 was in close contact with the surface. The deposition efficiency of approximately 8% was estimated

**Cyclic voltammetry (CV):** an electrochemical technique used to study the mechanisms and rates of oxidation-reduction processes in solution



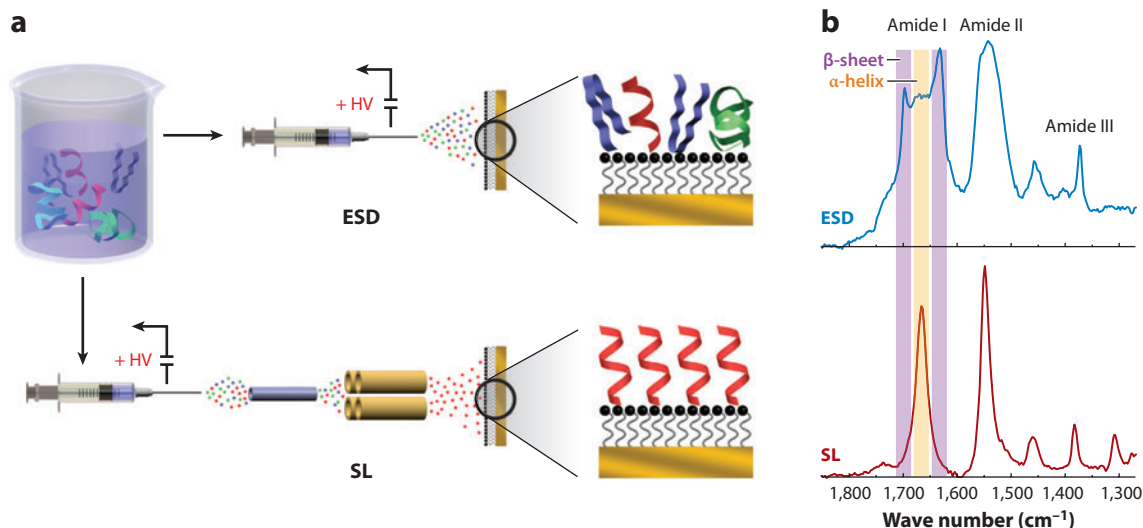


**Figure 3**

(a) Schematic drawing of (top) electro spray deposition (ESD) and (bottom) soft landing (SL) of peptide ions on self-assembled monolayer (SAM) surfaces. ESD of AcA<sub>15</sub>K from solution results in the formation of a peptide layer dominated by the  $\beta$ -sheet structure, and a stable  $\alpha$ -helical peptide layer on SAM surfaces is formed by SL. (b) Infrared reflection-absorption spectroscopy spectra of an AcA<sub>15</sub>K layer on the hydrocarbon SAM surface prepared by (top) ESD and (bottom) SL. The purple areas correspond to characteristic absorption of the  $\beta$ -sheet conformation, and the position of the  $\alpha$ -helical band is highlighted in gold. Reproduced from Reference 22 with permission. Copyright 2008, Wiley.

#### Primary structure:

the amino acid sequence of a protein

#### Epoxidation:

conversion of an unsaturated hydrocarbon into a cyclic three-atom ring ether termed an epoxide

#### $\beta$ -sheet:

a conformation consisting of strands connected laterally by at least two or three backbone hydrogen bonds that form a twisted, pleated sheet structure

#### $\alpha$ -helix:

a right-handed coiled or spiral structural conformation

from the CV data. Notably, this value reflects only the efficiency of RL of redox-active molecules because molecules that lose their redox activity cannot be observed with CV, and all loosely bound molecules are probably washed off the surface. The maximum RL efficiency was obtained with the kinetic energies of 100 V per charge for multiwalled carbon nanotubes (103) and 150 V per charge for gold surfaces (101). These experiments demonstrated that RL is a promising approach for the immobilization of redox-active peptides and proteins on electrodes.

The physical and chemical properties of thin peptide films on substrates are determined by both their primary and secondary structures. For example, immobilization of  $\alpha$ -helical peptides linked to various photosensitizers has been used to generate sensitive molecular photoswitches on solid supports (104). The large macrodipole of  $\alpha$ -helical peptides accelerates electron transfer between the photosensitizer and the metal surface. In addition,  $\alpha$ -helical peptides are effective enantioselective catalysts of some epoxidation reactions (105). SL and RL may be used for controlled preparation of  $\alpha$ -helical peptide films that cannot be prepared by absorption of a peptide from solution (22). Very different FTIR spectra were obtained following deposition of the AcA<sub>15</sub>K peptide from solution and from the gas phase (**Figure 3**). The spectrum obtained by electro spray deposition (ESD) is dominated by absorption bands that correspond to a mixture of the  $\beta$ -sheet,  $\alpha$ -helix, and other secondary structure motifs, whereas the spectrum obtained by SL yields a narrow amide I band that corresponds to the  $\alpha$ -helical conformation (22). Similarly, a narrow  $\alpha$ -helical amide I band was obtained following RL of AcA<sub>15</sub>K on an NHS-SAM. These findings indicate that whereas ESD resulted in the formation of a peptide layer dominated by the  $\beta$ -sheet structure, a stable  $\alpha$ -helical peptide layer was formed by both SL and RL, which demonstrates the utility of these techniques for the controlled preparation of conformationally selected peptide layers.

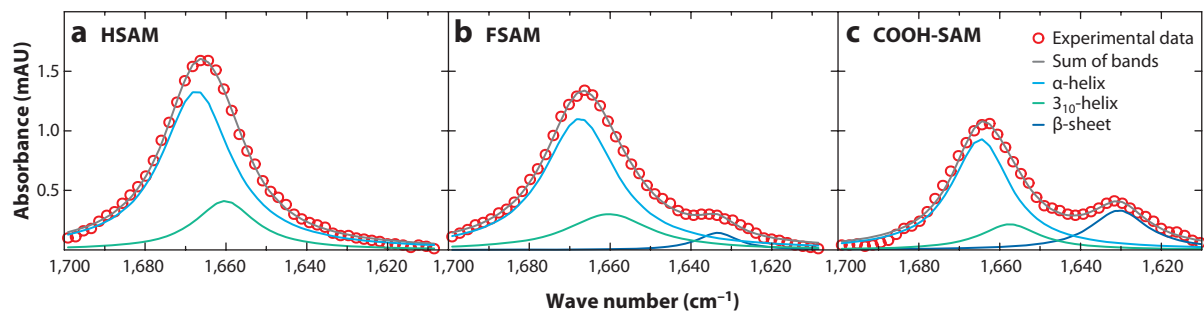


**Figure 4**

Amide I band region of infrared reflection-absorption spectroscopy spectra obtained following deposition of  $[\text{AcA}_{15}\text{K} + \text{H}]^+$  onto (a) hydrocarbon self-assembled monolayer (HSAM) surfaces, (b) fluorinated SAM (FSAM) surfaces, and (c) COOH-SAM surfaces. Experimental data are shown as open circles. Solid lines correspond to the  $\alpha$ -helix, the  $3_{10}$ -helix, and the  $\beta$ -sheet. Gray lines represent the sum of individual bands. Reproduced from Reference 106 with permission. Copyright 2010, Royal Society of Chemistry.

More recently, the effect of the chemical functionality of the SAM on the secondary structure of immobilized peptide molecules was examined by use of in situ FTIR. **Figure 4** shows FTIR spectra obtained following SL of  $\text{AcA}_{15}\text{K}$  onto hydrocarbon SAM (HSAM), FSAM, and COOH-SAM (106) surfaces. Clearly, the HSAM surface predominantly stabilizes the  $\alpha$ -helix, whereas a small fraction (5%) of  $\text{AcA}_{15}\text{K}$  deposited onto the FSAM and a larger fraction (22%) deposited onto the COOH-SAM adopt the  $\beta$ -sheet conformation. FTIR characterization demonstrated that there is a slow transition from the  $\alpha$ -helical to the  $\beta$ -sheet conformation on the COOH-SAM and no conformational change on the HSAM. Interestingly, almost identical FTIR spectra were obtained following SL of  $[\text{AcA}_{15}\text{K} + \text{H}]^+$  and  $[\text{AcKA}_{15} + \text{H}]^+$  ions, which adopt very different conformations in the gas phase; this finding indicates that for these rather small peptide systems, the initial gas-phase conformation of the ion is significantly altered by the surface.

## 2.2. Deposition of Proteins

SL may be utilized for the purification and immobilization of protein molecules for subsequent chemical characterization via a variety of analytical and biochemical approaches. In a pioneering study by Cooks and coworkers (23), protein arrays were prepared by SL of selected charge states of multiply protonated proteins on a gold surface. **Figure 5a** shows a photograph of a protein array obtained by SL of cytochrome *c*, lysozyme, insulin, and apomyoglobin at different positions on a surface. Mass spectra of proteins rinsed off the surface showed no signs of fragmentation during SL. An ESI spectrum of apomyoglobin rinsed off the surface (**Figure 5b**) contained only multiply charged ions of the protein, which confirmed intact deposition on the surface.

Retention of biological activity following SL was demonstrated for trypsin, lysozyme, and various kinases, which demonstrated the utility of this approach for selective preparation of protein arrays for potential application in high-throughput screening (23). The SL efficiency was independent of the selected charge state of the proteins. However, the collision energy and the properties of the substrate had a profound effect on protein SL. Maximum SL efficiency, defined as the amount of recovered material per number of ions directed at the surface, was observed for ion kinetic energies of approximately 3 eV per charge, whereas an order-of-magnitude-lower efficiency was obtained when the kinetic energy was increased to 10 eV per charge. Retention of biological activity was observed on liquid glycerol-based surfaces but not on SAMs (9). Similarly, the SL efficiency was approximately four times higher for liquid surfaces than for FSAM. The

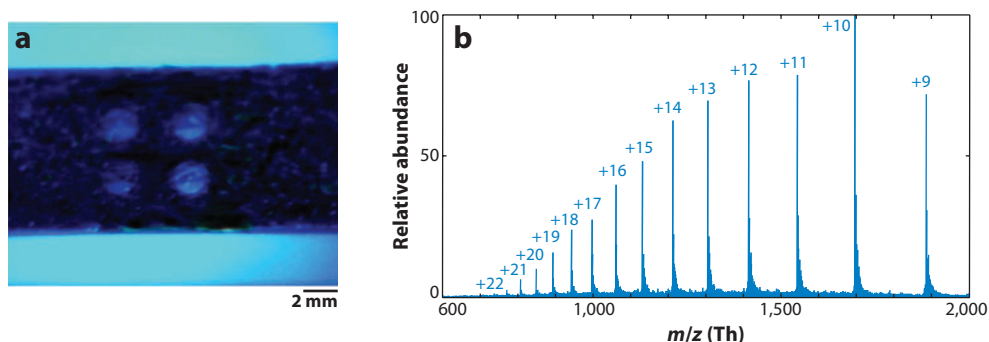


**Figure 5**

(a) Blue-light photograph of a microarray of four proteins that were soft-landed onto a gold substrate; each spot has a radius of 1 mm. (b) Electrospray ionization mass spectrum of soft-landed apomyoglobin following rinsing of the spot. Reproduced from Reference 23 with permission. Copyright 2003, American Association for the Advancement of Science.

difference in SL efficiency was attributed to partial charge retention by proteins deposited onto the FSAM surface, which resulted in charge accumulation on the substrate and prevented additional ions from approaching it.

In contrast, Volny et al. (58) reported a complete loss of charge for proteins soft-landed onto plasma-treated metal surfaces. The conformationally rigid trypsin and the flexible streptavidin were used as model systems in these authors' studies. Fluorescence detection was used to observe the removal of proteins upon rinsing. The protein ions that had soft-landed at nominal kinetic energies of 130 to 200 eV were arranged on the metal-oxide surface in two distinct layers. The top layer was readily washed off with a solvent, whereas the bottom layer remained tethered to the surface following extensive rinsing. The immobilized proteins showed 50–60% biological activity (58).

Surfaces and interfaces play an important role in modifying protein conformations through electrostatic and hydrophobic interactions. Conformational changes induced by protein-surface interactions were examined for various solid substrates, including metals (107), naturally occurring minerals, and SAMs (108–110). Immobilization of proteins has a dramatic effect on both the secondary structure and the function of adsorbed molecules. FTIR studies showed that protein deposition on the hydrophilic COOH-SAM results in higher yields of the  $\beta$ -sheet conformation and lower yields of the  $\alpha$ -helix, as compared with hydrophobic HSAM and FSAM surfaces.

Protein aggregation on surfaces is another interesting phenomenon (110–112) that may be studied with SL. The atomic force microscopy images in **Figure 6** show two-dimensional fractal clusters formed following deposition of multiply protonated bovine serum albumin onto a highly ordered pyrolytic graphite (HOPG) surface at low and high coverage (16). The degree of aggregation increases with coverage. The aggregates are formed both at step edges and on terraces, indicating that bovine serum albumin molecules are relatively immobile because of their strong interaction with the surface. Similar aggregation behavior was observed upon adsorption of fibrinogen onto the HOPG surface from solution (113). The proposed mechanism of aggregation assumes that, although hydrophobic regions of the protein interact with the HOPG surface, hydrophilic regions participate in the binding of other protein molecules in solution. SL is uniquely suited to study the propensity of protein aggregation on surfaces in the absence of solvent, which is important for obtaining a fundamental understanding of the factors that affect this process.

**Highly ordered pyrolytic graphite (HOPG):** a form of high-purity carbon with a smooth nonpolar surface



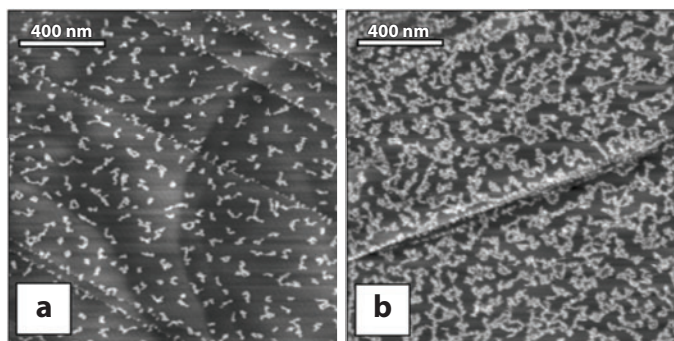


**Figure 6**

Atomic force microscopy topography of bovine serum albumin deposited on a highly ordered pyrolytic graphite surface under vacuum ( $10^{-6}$  mbar) at room temperature. Fractal aggregations formed by string-like particles were found on the surface, indicating that diffusion-limited aggregation occurred at (a) low and (b) high coverage. Reproduced from Reference 16 with permission. Copyright 2006, Wiley.

### 3. SOFT LANDING OF CLUSTERS

Deposition of nanoscale clusters onto surfaces may be used to create model catalytic systems that can provide insight into the factors that influence the effectiveness of heterogeneous catalysts (61). A large proportion of industrial catalysts consist of small metal particles supported on metal-oxide substrates (114). Consequently, a fundamental understanding of the effect of factors such as particle size, charge state, morphology, and interaction with the support on catalytic activity and selectivity is critical to rational design of improved catalytic materials (115). SL of mass-selected cluster ions allows one to investigate such factors with atomic-level precision, which is not possible with conventional reduction synthesis techniques (116). Moreover, nonthermal sources of cluster ions, such as laser vaporization and magnetron sputtering (3, 5), allow the generation of unique heterogeneous materials that cannot be easily produced in solution.

In the nanoscale-size regime, the addition or removal of single atoms often results in large changes in both the chemical and physical properties of clusters (117). For instance, the gas-phase reactivity of small (i.e., containing fewer than 20 atoms) anionic gold clusters with both carbon monoxide (CO) and oxygen ( $O_2$ ) exhibits large variations with size depending on whether the cluster has an open- or closed-shell electronic structure (**Figure 7**) (118). Similar intrinsic size effects have been observed in the reactivity of small metal clusters soft-landed onto thin metal-oxide supports (119–123). For instance, Heiz and coworkers (124) investigated the CO dissociation activity of monodisperse nickel ( $Ni_n$ , where  $n = 11, 20$ , and  $30$ ) clusters deposited onto magnesium oxide [ $MgO(110)$ ] surfaces. Using thermal desorption spectroscopy (TDS) combined with FTIR, the authors found that  $Ni_{30}$  clusters exhibit an intrinsic size effect that results in dissociation of CO at a lower temperature than on  $Ni_{11}$  or  $Ni_{20}$ . The increased activity was attributed to a higher proportion of sites on the  $Ni_{30}$  clusters that bind CO in a precursor state that leads to dissociation. More recently, Kaden and coworkers (40) examined the size-dependent CO oxidation activity of palladium ( $Pd_n$ , where  $n = 1, 2, 4, 7, 10, 16, 20$ , and  $25$ ) clusters soft-landed onto rutile  $TiO_2(110)$  surfaces. TDS experiments combined with X-ray photoemission spectroscopy revealed a nonmonotonic variation in CO oxidation reactivity with increasing cluster size that was strongly

**Catalytic activity:** the increase in the rate of a chemical reaction brought about by the presence of a catalyst

**Catalytic selectivity:** the amount of desired product formed in a chemical reaction in relation to the amount of undesired by-products formed

**Thermal desorption spectroscopy (TDS):** a method of observing desorbed molecules from a surface as the surface temperature is increased

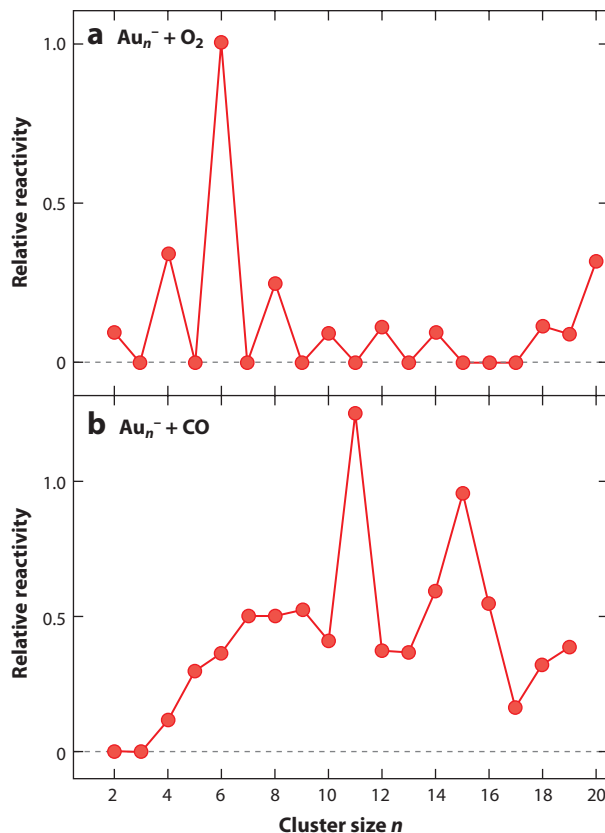


**Figure 7**

Compilation of experimental results from the literature on the relative reactivity of Au cluster anions in the adsorption reaction of one  $\text{O}_2$  and one CO molecule, respectively, as a function of the cluster size,  $n$ . (a) Reactions between  $\text{Au}_n^-$  and  $\text{O}_2$ . For comparison, all data are normalized to the reactivity of  $\text{Au}_6^-$ . (b) Reactions between  $\text{Au}_n^-$  and CO. Again, the data are normalized to the reactivity of  $\text{Au}_6^-$  toward  $\text{O}_2$ . Reproduced from Reference 118 with permission. Copyright 2005, Elsevier.

correlated with the Pd 3d electron-binding energy (**Figure 8**). Lower CO oxidation reactivity was associated with larger Pd 3d electron-binding energies, which indicate the presence of stable valence electronic structures of the supported clusters.

SL also has been used to determine how defects in support materials influence catalytic activity. For example, Yoon et al. (125) demonstrated that F-center surface defects in the MgO support are critical to the enhanced catalytic activity of soft-landed  $\text{Au}_8^+$  clusters toward the oxidation of CO to carbon dioxide ( $\text{CO}_2$ ). TDS revealed a significantly enhanced yield of  $\text{CO}_2$  at low temperature (140 K) for  $\text{Au}_8$  clusters supported on defect-rich MgO substrates compared with surfaces that were defect-poor. The FTIR spectra of CO molecules bound to the  $\text{Au}_8/\text{MgO}$  (defect-rich) surface indicated a significant redshift of the CO band resulting from electron back-donation from the cluster to the CO antibonding orbitals. Theoretical calculations confirm that the electron density trapped in the F-center defect of the MgO surface is partially transferred to the supported  $\text{Au}_8$  cluster (126) and that this density on the cluster then activates the CO bond, resulting in enhanced oxidation reactivity. In addition, the authors of this study proposed that the F-center defects on

**F-center defect:** a color-center defect in metal oxides that consists of two electrons trapped in an oxygen vacancy

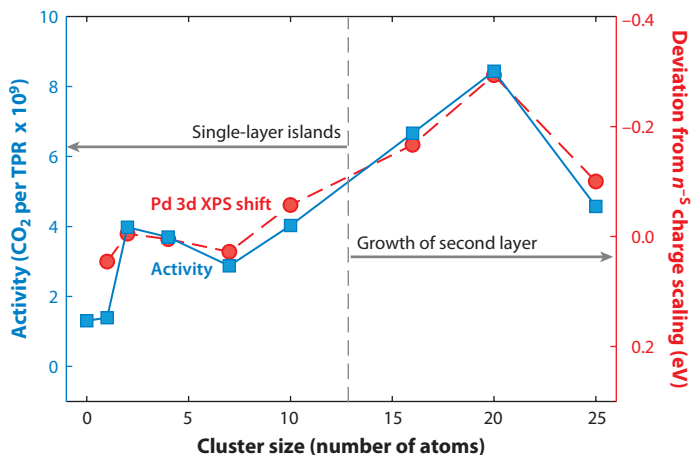


**Figure 8**

CO oxidation activity observed during temperature-programmed reaction (TPR) (*left axis*) compared with shifts in the Pd 3d electron-binding energy, relative to expectations from smooth bulk scaling (*right axis*), as a function of cluster size. Abbreviation: XPS, X-ray photoemission spectroscopy. Reproduced from Reference 40 with permission. Copyright 2009, American Association for the Advancement of Science.

the MgO surface anchor the deposited Au<sub>8</sub> clusters (**Figure 9**), thereby preventing their migration and agglomeration into larger inactive particles.

SL of size-selected clusters has also been used to identify new catalytic materials with enhanced activity toward industrially relevant reactions. For example, although propylene oxide is an important intermediate used in the production of chemicals, until recently no direct method for the oxidation of propylene to propylene oxide by use of O<sub>2</sub> had been developed. By using SL combined with temperature-programmed reaction experiments, Lei and coworkers (127) found that Ag<sub>3</sub> clusters deposited onto alumina supports catalyze the partial oxidation of propylene to propylene oxide, with negligible formation of the unwanted by-product CO<sub>2</sub>. Theoretical calculations indicate that, upon exposure to O<sub>2</sub>, an oxidized Ag<sub>3</sub>O trimer forms on the surface. This trimer

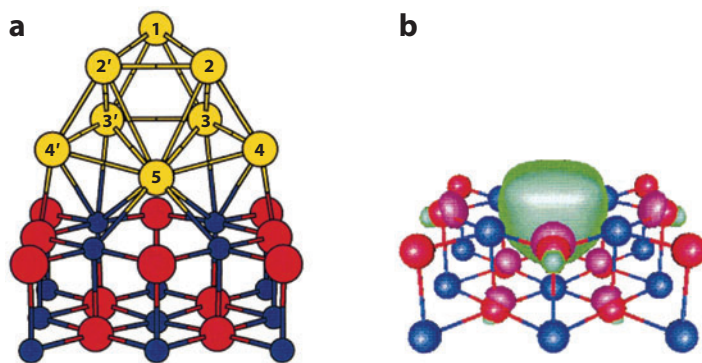


**Figure 9**

(*a*) View of the energy-optimal structure of Au<sub>8</sub> particles adsorbed on the MgO(100) surface containing an O-vacancy F-center. (*b*) Isovalue surface of the 2e<sup>-</sup> F-center wave function showing the electron density trapped in the O vacancy. Reproduced from Reference 126 with permission. Copyright 2006, American Chemical Society.

**Transmission electron microscopy (TEM):** a microscopy technique in which a beam of electrons is transmitted through an ultrathin specimen, interacts with the specimen as it passes through, and creates an image that is then magnified

exhibits enhanced activity and selectivity toward the formation of propylene oxide due to its open-shell electronic structure. In another publication (128), the same group examined the effect of two common contaminants, hydrogen ( $\text{H}_2$ ) and water ( $\text{H}_2\text{O}$ ), on the catalytic activity and selectivity of  $\text{Au}_{6-10}$  clusters soft-landed onto alumina toward the epoxidation of propene. The authors found that the presence of  $\text{H}_2$  or  $\text{H}_2\text{O}$  in the reactant stream results in a significantly higher selectivity toward propene oxide, rather than toward the unwanted by-product acrolein. Density functional theory calculations indicate that the  $\text{H}_2$  and  $\text{H}_2\text{O}$  contaminants maintain a hydroxy-terminated alumina surface that is critical to the enhanced selectivity toward propene oxide. Importantly, this study demonstrated that the expensive and dangerous  $\text{H}_2$ , which is normally used to enhance the selectivity of the reaction, may be replaced by the abundant and safe  $\text{H}_2\text{O}$ .

One of the unique advantages of nonthermal sources of cluster ions is that they can produce materials that are currently not accessible through solution-phase synthesis. Therefore, in addition to the properties of pure metal clusters, the properties of heterogeneous metal carbide, sulfide, and oxide clusters soft-landed onto various support materials have been investigated. For example, in 1992 Castleman and coworkers (129) discovered metallocarbohedrene ( $\text{M}_8\text{C}_{12}$ ) clusters in the gas phase. Several years later, in an effort to isolate these clusters in the condensed phase, the same group investigated the SL of  $\text{Zr}_8\text{C}_{12}^+$  clusters, which were generated by laser vaporization of a metal-graphite target, onto carbon-covered grids (75). The resulting materials were studied by high-resolution transmission electron microscopy (TEM), which demonstrated that, under hard landing conditions, the metal-carbon clusters rearrange to produce the bulk metal carbide and that, under SL conditions, a face-centered cubic (FCC) structure with a lattice parameter of approximately 1.5 nm is formed; this structure arises from cluster assembly on the surface.

In a similar vein, Lightstone and coworkers (42) examined the SL of molybdenum sulfide ( $\text{Mo}_4\text{S}_6^+$ ) clusters, generated by magnetron sputtering, onto Au(111) surfaces. The interest in  $\text{Mo}_4\text{S}_6^+$  stems from its widespread application as a hydrodesulfurization catalyst. TDS experiments combined with Auger spectroscopy revealed that the clusters remain isolated on the surface up to coverages of approximately 0.15 monolayer, whereas at higher exposures, cluster crowding and island formation are observed. Heating of the substrate to 500 K caused cluster diffusion and aggregation on the Au(111) surface. Using density functional theory calculations, the authors predicted the optimum binding geometry of the  $\text{Mo}_4\text{S}_6^+$  cluster to the surface and showed that CO molecules bind preferentially to the Mo atom top site, as opposed to the side sites.

The influence of cluster-cluster and cluster-surface interactions on the self-organization and agglomeration/sintering of particles on surfaces has also been investigated with SL techniques. In an early publication, Goldby et al. (130) investigated the diffusion and aggregation of silver clusters containing between 50 and 250 atoms deposited onto graphite surfaces. Employing scanning electron microscopy (SEM), the authors found that for all sizes, the clusters are mobile on the surface and tend to coalesce into larger three-dimensional particles with a consistent diameter of approximately 14 nm. These 14-nm particles were observed to be mobile and to condense into larger aggregates. In addition, the impact angle of the clusters with the surface influenced the size distribution of the larger aggregates: Impact angles further from surface normal resulted in larger islands, due to the enhanced initial surface mobility of the deposited clusters.

More recently, Tainoff et al. (131) reported the self-organization of platinum nanoclusters into dense catalytic arrays. In this study, a size-selected distribution of platinum clusters ranging from 2 to 3 nm in diameter were produced by laser vaporization and deposited at low energy onto HOPG surfaces. TEM images revealed multiple surface regions containing highly ordered arrays of platinum clusters (**Figure 10**). In contrast, when the entire size distribution of platinum clusters was deposited, no ordered arrays were observed with TEM. Furthermore, self-organization

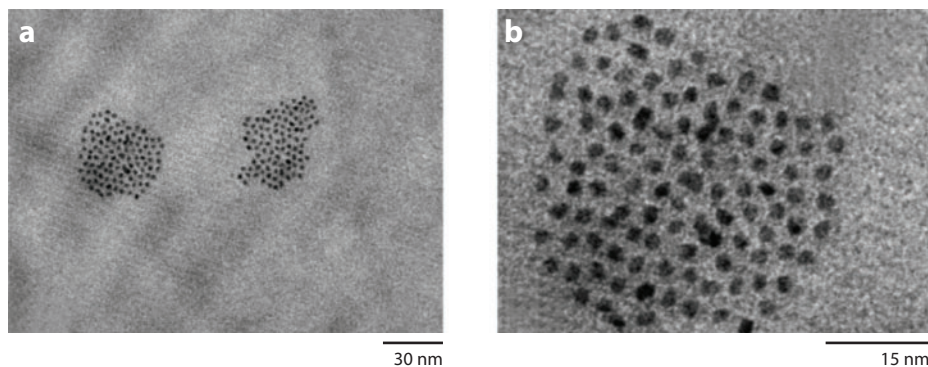


**Figure 10**

Typical transmission electron microscopy morphologies of platinum cluster (2–3-nm) arrays obtained at different magnifications. Reproduced from Reference 131 with permission. Copyright 2008, American Chemical Society.

appears to depend on the chemical identity of the cluster, given that equivalent-size gold clusters exhibit no formation of arrays on the surface.

Several researchers have investigated the RL, or pinning, of small metal clusters on substrates to create isolated species on the surface that do not diffuse and agglomerate. For instance, Kenny et al. (132) examined the implantation depth of size-selected  $\text{Ag}_7^-$  clusters into graphite surfaces as a function of kinetic energy. Using scanning tunneling microscopy and molecular dynamics simulations, the authors found that for small clusters, the implantation depth is proportional to the velocity of the bombarding cluster, rather than the kinetic energy. Additional studies demonstrated that for size-selected clusters, there is a critical size-dependent impact energy that must be exceeded for clusters to become pinned to the surface (133). Moreover, for larger clusters containing between 20 and 200 atoms, the implantation depth varied linearly as a function of both the cluster size and the kinetic energy. There are various applications for small metal clusters pinned to surfaces in this fashion. For instance, Leung et al. (134) showed that  $\text{Au}_{17}$  clusters pinned to graphite surfaces may be utilized to immobilize proteins.

#### 4. SOFT LANDING OF ORGANOMETALLIC COMPLEXES

Deposition of metal-ligand complexes onto surfaces may be used to prepare high-purity thin films of organometallics. These materials are of interest to the evolving field of hybrid organic-inorganic interfaces (135). More specifically, solution-phase organometallic catalysts exhibit high selectivity toward desired products due to their single-site nature but are difficult to separate from products and remaining reactants because they are mixed together in solution (136). In comparison, solid-phase heterogeneous catalysts often contain various active sites, which reduce catalytic selectivity but remain widely employed because they enable easy recovery of products. Recently, investigators have attempted to exploit the best aspects of both materials by immobilizing organometallic complexes on inorganic supports (137). SL and RL of mass-selected ions constitute a novel approach for the preparation of surface-bound organometallics that uses fewer raw materials and solvents and avoids the purification steps involved with solution-phase synthesis techniques.

The feasibility of generating and transferring gas-phase organometallic ions to surfaces intact was demonstrated by Judai et al. (47), who used collisions of  $\text{V}_n(\text{benzene})_m^+$  cluster ions with a polycrystalline gold surface cooled to 18 K and covered with approximately 30 monolayers of argon. FTIR spectra of the surface taken 1 h after deposition indicated the presence of neutral



**Collision-induced dissociation (CID):** a method of fragmenting molecular ions in the gas phase through acceleration and collision with a neutral gas molecule

$V(\text{benzene})_2$  complexes with a sandwich-like structure. This study, therefore, established that IR spectroscopy of ions deposited into an inert matrix may be used to obtain information about the structures of organometallic clusters generated in the gas phase. Subsequently, Mitsui et al. (46) investigated the SL of the same  $V(\text{benzene})_2^+$  cluster ions onto clean gold surfaces and long-chain alkanethiolate SAMs on gold. TDS experiments revealed significantly stronger binding of the cluster ions to the surface of the SAM in comparison to the clean gold surface, which was attributed to penetration of the complexes into the alkanethiol matrix. In addition, IR spectra of the surfaces established that the  $V(\text{benzene})_2$  clusters have no preferential orientation on clean gold but are oriented with the molecular axis tilted  $70\text{--}80^\circ$  on the SAM surface.

Charge reduction has been examined for the deposition of  $\text{Co}^{\text{III}}(\text{salen})^+$  and  $\text{Mn}^{\text{III}}(\text{salen})^+$  [where salen refers to  $N,N'$ -ethylenebis(salicylideneaminato)] complexes onto HSAM and FSAM surfaces (86). In contrast with protonated molecules that undergo proton loss upon immobilization on the surface (97), charge loss by deposited organometallic complexes and metal clusters on thin insulating films requires electron transfer through the insulating layer to the deposited species. Charge retention by a significant fraction of precursor ions on the FSAM and complete neutralization on the HSAM were observed. The results demonstrate efficient electron transfer from gold to the complex deposited onto the HSAM and inefficient, if any, electron transfer on the FSAM surface.

SL may be employed to create catalytically active materials through immobilization of metal-ligand complexes on SAM surfaces. For example, in a recent study, Peng et al. (49) examined the oxidation-reduction chemistry of organometallic metal-salen complexes soft-landed onto inert FSAM surfaces. Metal-salen complexes are widely employed as solution-phase catalysts to promote reactions such as olefin epoxidation and ring-opening polymerization of cyclic carbonates (138). Furthermore, electrochemical studies in the solution phase have shown that  $\text{VO}(\text{salen})$  reacts in acidic media to form  $\text{VO}(\text{salen})^+$  and deoxygenated  $\text{V}(\text{salen})^+$ ; the latter is an important intermediate in the catalytic reduction of  $\text{O}_2$  to  $\text{H}_2\text{O}$  (139). The authors demonstrated, through SL of  $\text{VO}(\text{salen})^+$  and a proton donor,  $[\text{Ni}(\text{salen})+\text{H}]^+$ , into an FSAM surface, that it is possible to observe the same acid-mediated reduction of  $\text{VO}(\text{salen})^+$  to  $\text{V}(\text{salen})^+$  in thin films produced by ion deposition. Using in situ TOF-SIMS, they tracked the relative abundance of the reactants and products on the surface in vacuum over a period of several days. A pronounced growth in the relative abundance of  $\text{V}(\text{salen})^+$  and  $\text{Ni}(\text{salen})^+$  with time was observed, indicating that  $[\text{Ni}(\text{salen})+\text{H}]^+$  donates its proton to the monolayer forming an acidic environment, which then mediates the deoxygenation of  $\text{VO}(\text{salen})^+$  to  $\text{V}(\text{salen})^+$ . Furthermore, the authors showed that (a) exposure to  $\text{O}_2$  regenerates the original  $\text{VO}(\text{salen})$  complex, thereby completing a full redox cycle, and (b) this cycle may occur multiple times, which is consistent with catalytic behavior.

In a subsequent study, Johnson & Laskin (50) demonstrated the feasibility of preparing surface immobilized organometallic catalysts through gas-phase ligand stripping and RL of mass-selected ions. In this study, ruthenium tris(bipyridine)  $[\text{Ru}(\text{bpy})_3]^{2+}$  dications were reactively landed onto  $\text{COOH-SAMs}$  forming strongly bound  $\text{Ru}(\text{bpy})_2$ -thiol adducts. In situ TOF-SIMS showed that if one of the bipyridine ligands is removed through gas-phase collision-induced dissociation (CID) prior to deposition, a significantly larger yield of the surface immobilized complexes can be obtained. Therefore, through the use of a mass spectrometer, CID can be employed to convert a relatively inert closed-shell organometallic complex into a highly reactive open-shell species that exhibits enhanced activity toward RL (**Figure 11**). In addition, if the prepared substrates are exposed to the gaseous reagents  $\text{O}_2$  and  $\text{C}_2\text{H}_4$ , the immobilized complexes undergo a redox cycle consistent with catalytic behavior. SL, therefore, may be used to prepare and isolate high-purity thin films of organometallic complexes, to achieve orientational control over the resulting materials, and to generate catalytically active substrates.

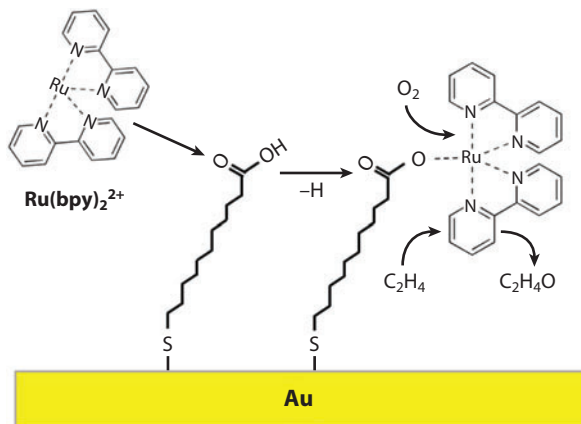


**Figure 11**

Graphical representation of the immobilization of  $\text{Ru}(\text{bpy})_2^{2+}$  on COOH-terminated self-assembled monolayer surfaces through gas-phase ligand stripping and reactive landing of mass-selected ions. Reproduced from Reference 50 with permission. Copyright 2010, Wiley.

## 5. FUTURE OUTLOOK

Preparatory mass spectrometry using SL and RL of mass-selected ions is uniquely suited for the controlled immobilization of complex molecules on substrates. However, the ability to prepare functional materials using these techniques is limited because typical ion currents obtained using ESI are two to three orders of magnitude lower than those utilized in micro- and nanofabrication. Development of high-transmission bright ESI and laser-based ion sources is an important prerequisite for converting SL and RL into practical microfabrication approaches. In addition, combining SL with ion-mobility separation will enable precise control of both the primary and secondary structures of deposited species, which is important both for practical applications and for understanding the effect of the surface on the secondary structure of immobilized molecules. Moreover, the unique capabilities of the mass spectrometer may be used to manipulate molecules in the gas phase, through either CID or ion-molecule reactions, to generate new species that are not obtainable through solution-phase synthesis.

Immobilization of peptides and proteins by use of SL and RL enables detailed studies of the interactions of biomolecules with surfaces in the absence of solvent. Such studies provide information about binding energies, the kinetics of conformational changes, and the agglomeration of proteins and other complex molecules following adsorption. Also, deposition of size-selected clusters allows one to study, with atomic-level precision, the influence of factors such as size, morphology, charge state, and interaction with the support. SL and RL of metal-ligand complexes constitute a novel approach for the preparation of organometallic thin films that are catalytically active.

Preparation of materials relies on a fundamental understanding of structure-function relationships. Sensitive characterization is essential for in situ analysis of the effect of the surface on the higher-order structure and the activity of deposited species. Most existing surface-characterization techniques often provide limited structural information and are not always capable of in situ, real-time analysis of modified surfaces. Future applications will explore the utility of nonlinear surface spectroscopy techniques for the determination of conformations and orientation of biomolecules and organometallic complexes that are immobilized on solid supports.

## SUMMARY POINTS

1. SL helps overcome the limitations of MLD for the preparation of thin films of complex molecules on solid supports.
2. The advantages of SL include highly specific preparation of deposited species; deposition of uniform films; patterning; and deposition of a broad range of analytes, including biomolecules, clusters, and organometallic complexes.
3. Nonthermal ionization sources combined with SL instrumentation provide access to unique materials that cannot be easily produced through conventional techniques.
4. RL enables precise control of the kinetic energy of the ion, which leads to high yields of interfacial reactions.
5. SL and RL may be used to prepare novel biomaterials.
6. SL of proteins enables the preparation of protein arrays and the purification of proteins for subsequent characterization and provides a new means for studying aggregation and conformational transitions of adsorbed proteins.
7. SL of size-selected clusters may be used to create model catalytic systems that provide insight into the factors that influence the activity and selectivity of heterogeneous catalysts.
8. RL may be used to tether metal-ligand complexes to substrates, thereby creating hybrid surface organometallic catalysts that combine the most beneficial aspects of homogeneous and heterogeneous catalysts.

## DISCLOSURE STATEMENT

The authors are not aware of any affiliations, memberships, funding, or financial holdings that might be perceived as affecting the objectivity of this review.

## ACKNOWLEDGMENTS

The authors acknowledge support from the Chemical Sciences Division, Office of Basic Energy Sciences, of the U.S. Department of Energy (DOE); the Laboratory Directed Research and Development Program at the Pacific Northwest National Laboratory (PNNL); and the W.R. Wiley Environmental Molecular Sciences Laboratory, a national scientific user facility sponsored by the DOE. PNNL is operated by Battelle for DOE. The authors also are grateful to Prof. Graham Cooks, Prof. Wen Ping Peng, Dr. Omar Hadjar, and Dr. Peng Wang for their contribution to the development of the concepts presented in this review.

## LITERATURE CITED

1. Fenn JB, Mann M, Meng CK, Wong SF, Whitehouse CM. 1990. Electrospray ionization—principles and practice. *Mass Spectrom. Rev.* 9:37–70
2. Fenn JB, Mann M, Meng CK, Wong SF, Whitehouse CM. 1989. Electrospray ionization for mass spectrometry of large biomolecules. *Science* 246:64–71
3. Milani P, Deheer WA. 1990. Improved pulsed laser vaporization source for production of intense beams of neutral and ionized clusters. *Rev. Sci. Instrum.* 61:1835–38

4. Wagner RL, Vann WD, Castleman AW. 1997. A technique for efficiently generating bimetallic clusters. *Rev. Sci. Instrum.* 68:3010–13
5. Pratontep S, Carroll SJ, Xirouchaki C, Streun M, Palmer RE. 2005. Size-selected cluster beam source based on radio frequency magnetron plasma sputtering and gas condensation. *Rev. Sci. Instrum.* 76:045103
6. Xirouchaki C, Palmer RE. 2004. Deposition of size-selected metal clusters generated by magnetron sputtering and gas condensation: a progress review. *Philos. Trans. R. Soc. Lond. B* 362:117–24
7. Franchetti V, Solka BH, Baitinger WE, Amy JW, Cooks RG. 1977. Soft landing of ions as a means of surface modification. *Int. J. Mass Spectrom. Ion Process.* 23:29–35
8. Lapack MA, Pachuta SJ, Busch KL, Cooks RG. 1983. Surface modification by soft landing of reagent beams. *Int. J. Mass Spectrom. Ion Process.* 53:323–26
9. Gologan B, Takats Z, Alvarez J, Wiseman JM, Talaty N, et al. 2004. Ion soft-landing into liquids: protein identification, separation, and purification with retention of biological activity. *J. Am. Soc. Mass Spectrom.* 15:1874–84
10. Gologan B, Green JR, Alvarez J, Laskin J, Cooks RG. 2005. Ion/surface reactions and ion soft-landing. *Phys. Chem. Chem. Phys.* 7:1490–500
11. Blake TA, Zheng OY, Wiseman JM, Takats Z, Guymon AJ, et al. 2004. Preparative linear ion trap mass spectrometer for separation and collection of purified proteins and peptides in arrays using ion soft landing. *Anal. Chem.* 76:6293–305
12. Volny M, Elam WT, Ratner BD, Turecek F. 2007. Enhanced in-vitro blood compatibility of 316L stainless steel surfaces by reactive landing of hyaluronan ions. *J. Biomed. Mater. Res. B* 80B:505–10
13. Rader HJ, Rouhanipour A, Talarico AM, Palermo V, Samori P, Mullen K. 2006. Processing of giant graphene molecules by soft-landing mass spectrometry. *Nat. Mater.* 5:276–80
14. Heiz U, Schneider WD. 2001. Size-selected clusters on solid surfaces. *Crit. Rev. Solid State Mater. Sci.* 26:251–90
15. Vajda S, Winans RE, Elam JW, Lee BD, Pellin MJ, et al. 2006. Supported gold clusters and cluster-based nanomaterials: characterization, stability and growth studies by in situ GISAXS under vacuum conditions and in the presence of hydrogen. *Top. Catal.* 39:161–66
16. Rauschenbach S, Stadler FL, Lunedei E, Malinowski N, Koltsov S, et al. 2006. Electrospray ion beam deposition of clusters and biomolecules. *Small* 2:540–47
17. Cheng HP, Landman U. 1993. Controlled deposition, soft landing, and glass-formation in nanocluster-surface collisions. *Science* 260:1304–7
18. Bittner AM. 2006. Clusters on soft matter surfaces. *Surf. Sci. Rep.* 61:383–428
19. Rauschenbach S, Vogelgesang R, Malinowski N, Gerlach JW, Benyoucef M, et al. 2009. Electrospray ion beam deposition: soft-landing and fragmentation of functional molecules at solid surfaces. *Am. Chem. Soc. Nano* 3:2901–10
20. Saf R, Goriup M, Steindl T, Hamedinger TE, Sandholzer D, Hayn G. 2004. Thin organic films by atmospheric-pressure ion deposition. *Nat. Mater.* 3:323–29
21. Nanita SC, Takats Z, Cooks RG. 2004. Chiral enrichment of serine via formation, dissociation, and soft-landing of octameric cluster ions. *J. Am. Soc. Mass Spectrom.* 15:1360–65
22. Wang P, Laskin J. 2008. Helical peptide arrays on self-assembled monolayer surfaces through soft and reactive landing of mass-selected ions. *Angew. Chem. Int. Ed.* 47:6678–80
23. Ouyang Z, Takats Z, Blake TA, Gologan B, Guymon AJ, et al. 2003. Preparing protein microarrays by soft-landing of mass-selected ions. *Science* 301:1351–54
24. Evans C, Wade N, Pepi F, Strossman G, Schuerlein T, Cooks RG. 2002. Surface modification and patterning using low-energy ion beams: Si-O bond formation at the vacuum/adsorbate interface. *Anal. Chem.* 74:317–23
25. Siekmann HR, Luder C, Faehrmann J, Lutz HO, Meiwesbroer KH. 1991. The pulsed-arc cluster ion-source (Pacis). *Z. Phys. D* 20:417–20
26. Goldby IM, von Issendorff B, Kuipers L, Palmer RE. 1997. Gas condensation source for production and deposition of size-selected metal clusters. *Rev. Sci. Instrum.* 68:3327–34
27. Song QY, Smith SA, Gao L, Xu W, Volny M, et al. 2009. Mass selection of ions from beams using waveform isolation in radiofrequency quadrupoles. *Anal. Chem.* 81:1833–40

28. Mayer PS, Turecek F, Lee HN, Scheidemann AA, Olney TN, et al. 2005. Preparative separation of mixtures by mass spectrometry. *Anal. Chem.* 77:4378–84
29. Kemper P, Kolmakov A, Tong X, Lilach Y, Benz L, et al. 2006. Formation, deposition and examination of size selected metal clusters on semiconductor surfaces: an experimental setup. *Int. J. Mass Spectrom.* 254:202–9
30. Alvarez J, Cooks RG, Barlow SE, Gaspar DJ, Futrell JH, Laskin J. 2005. Preparation and in situ characterization of surfaces using soft landing in a Fourier transform ion cyclotron resonance mass spectrometer. *Anal. Chem.* 77:3452–60
31. Peng WP, Goodwin MP, Nie ZX, Volny M, Zheng OY, Cooks RG. 2008. Ion soft landing using a rectilinear ion trap mass spectrometer. *Anal. Chem.* 80:6640–49
32. Nie ZX, Li GT, Goodwin MP, Gao L, Cyriac J, Cooks RG. 2009. In situ SIMS analysis and reactions of surfaces prepared by soft landing of mass-selected cations and anions using an ion trap mass spectrometer. *J. Am. Soc. Mass Spectrom.* 20:949–56
33. Kim H, Lee HBR, Maeng WJ. 2009. Applications of atomic layer deposition to nanofabrication and emerging nanodevices. *Thin Solid Films* 517:2563–80
34. Du Y, George SM. 2007. Molecular layer deposition of nylon 66 films examined using in situ FTIR spectroscopy. *J. Phys. Chem. C* 111:8509–17
35. Yoshimura T, Tatsura S, Sotoyama W. 1991. Polymer-films formed with monolayer growth steps by molecular layer deposition. *Appl. Phys. Lett.* 59:482–84
36. Loscutoff PW, Zhou H, Clendenning SB, Bent SF. 2010. Formation of organic nanoscale laminates and blends by molecular layer deposition. *Am. Chem. Soc. Nano* 4:331–41
37. George SM, Yoon B, Dameron AA. 2009. Surface chemistry for molecular layer deposition of organic and hybrid organic-inorganic polymers. *Acc. Chem. Res.* 42:498–508
38. Miller SA, Luo H, Pachuta SJ, Cooks RG. 1997. Soft-landing of polyatomic ions at fluorinated self-assembled monolayer surfaces. *Science* 275:1447–50
39. Heiz U, Vanolli F, Trento L, Schneider WD. 1997. Chemical reactivity of size-selected supported clusters: an experimental setup. *Rev. Sci. Instrum.* 68:1986–94
40. Kaden WE, Wu TP, Kunkel WA, Anderson SL. 2009. Electronic structure controls reactivity of size-selected Pd clusters adsorbed on TiO<sub>2</sub> surfaces. *Science* 326:826–29
41. Carroll SJ, Pratontep S, Streun M, Palmer RE, Hobday S, Smith R. 2000. Pinning of size-selected Ag clusters on graphite surfaces. *J. Chem. Phys.* 113:7723–27
42. Lightstone JM, Patterson MJ, Liu P, Lofaro JC, White MG. 2008. Characterization and reactivity of the Mo<sub>4</sub>S<sub>6</sub><sup>+</sup> cluster deposited on Au(111). *J. Phys. Chem. C* 112:11495–506
43. Löffler D, Bajales N, Cudaj M, Weis P, Lebedkin S, et al. 2009. Non-IPR C<sub>60</sub> solids. *J. Chem. Phys.* 130:164705
44. Kaiser B, Bernhardt TM, Stegemann B, Opitz J, Rademann K. 1999. Bimodal distribution in the fragmentation behavior of small antimony clusters Sb<sub>x</sub><sup>+</sup> (*x* = 3–12) scattered from a highly oriented pyrolytic graphite surface. *Phys. Rev. Lett.* 83:2918–21
45. Yamaguchi W, Yoshimura K, Tai Y, Maruyama Y, Igarashi K, et al. 1999. Energy-controlled depositions of size-selected silver nanoparticles on HOPG substrates. *Chem. Phys. Lett.* 311:341–45
46. Mitsui M, Nagaoka S, Matsumoto T, Nakajima A. 2006. Soft-landing isolation of vanadium-benzene sandwich clusters on a room-temperature substrate using *n*-alkanethiolate self-assembled monolayer matrixes. *J. Phys. Chem. B* 110:2968–71
47. Judai K, Sera K, Amatsutsumi S, Yagi K, Yasuike T, et al. 2001. A soft-landing experiment on organometallic cluster ions: infrared spectroscopy of V(benzene)<sub>2</sub> in Ar matrix. *Chem. Phys. Lett.* 334:277–84
48. Johnson GE, Lysonski M, Laskin J. 2010. In situ reactivity and TOF-SIMS analysis of surfaces prepared by soft and reactive landing of mass-selected ions. *Anal. Chem.* 82:5718–27
49. Peng WP, Johnson GE, Fortmeyer IC, Wang P, Hadjar O, et al. 2011. Redox chemistry in thin films of organometallic complexes prepared using ion soft landing. *Phys. Chem. Chem. Phys.* 13:267–75
50. Johnson GE, Laskin J. 2010. Preparation of surface organometallic catalysts by gas-phase ligand stripping and reactive landing of mass-selected ions. *Chem. Eur. J.* 16:14433–38



51. Alvarez J, Futrell JH, Laskin J. 2006. Soft-landing of peptides onto self-assembled monolayer surfaces. *J. Phys. Chem. A* 110:1678–87
52. Yang XL, Mayer PS, Turecek F. 2006. Preparative separation of a multicomponent peptide mixture by mass spectrometry. *J. Mass Spectrom.* 41:256–62
53. Hadjar O, Wang P, Futrell JH, Laskin J. 2009. Effect of the surface on charge reduction and desorption kinetics of soft landed peptide ions. *J. Am. Soc. Mass Spectrom.* 20:901–6
54. Wang P, Hadjar O, Gassman PL, Laskin J. 2008. Reactive landing of peptide ions on self-assembled monolayer surfaces: an alternative approach for covalent immobilization of peptides on surfaces. *Phys. Chem. Chem. Phys.* 10:1512–22
55. Laskin J, Wang P, Hadjar O. 2008. Soft-landing of peptide ions onto self-assembled monolayer surfaces: an overview. *Phys. Chem. Chem. Phys.* 10:1079–90
56. Wang P, Hadjar O, Laskin J. 2007. Covalent immobilization of peptides on self-assembled monolayer surfaces using soft-landing of mass-selected ions. *J. Am. Chem. Soc.* 129:8682–83
57. Laskin J, Wang P, Hadjar O, Futrell JH, Alvarez J, Cooks RG. 2007. Charge retention by peptide ions soft-landed onto self-assembled monolayer surfaces. *Int. J. Mass Spectrom.* 265:237–43
58. Volny M, Elam WT, Branca A, Ratner BD, Turecek F. 2005. Preparative soft and reactive landing of multiply charged protein ions on a plasma-treated metal surface. *Anal. Chem.* 77:4890–96
59. Feng BB, Wunschel DS, Masselon CD, Pasa-Tolic L, Smith RD. 1999. Retrieval of DNA using soft-landing after mass analysis by ESI-FTICR for enzymatic manipulation. *J. Am. Chem. Soc.* 121:8961–62
60. Siuzdak G, Bothner B, Yeager M, Brugidou C, Fauquet CM, et al. 1996. Mass spectrometry and viral analysis. *Chem. Biol.* 3:45–48
61. Heiz U, Bullock EL. 2004. Fundamental aspects of catalysis on supported metal clusters. *J. Mater. Chem.* 14:564–77
62. Heiz U, Abbet S, Sanchez A, Schneider WD, Hakkinen H, Landman U. 2001. Chemical reactions on size-selected clusters on surfaces. *Phys. Chem. Clust.* 117:87–98
63. Abbet S, Judai K, Klinger L, Heiz U. 2002. Synthesis of monodispersed model catalysts using softlanding cluster deposition. *Pure Appl. Chem.* 74:1527–35
64. Nagaoka S, Matsumoto T, Ikemoto K, Mitsui M, Nakajima A. 2007. Soft-landing isolation of multi-decker V<sub>2</sub>(benzene)<sub>3</sub> complexes in an organic monolayer matrix: an infrared spectroscopy and thermal desorption study. *J. Am. Chem. Soc.* 129:1528–29
65. Nagaoka S, Ikemoto K, Matsumoto T, Mitsui M, Nakajima A. 2008. Soft-landing isolation of gas-phase-synthesized transition metal–benzene complexes into a fluorinated self-assembled monolayer matrix. *J. Phys. Chem. C* 112:15824–31
66. Nagaoka S, Ikemoto K, Matsumoto T, Mitsui M, Nakajima A. 2008. Thermal and hyperthermal collision-energy depositions of transition metal–benzene sandwich complexes onto a self-assembled *n*-octadecanethiol monolayer. *J. Phys. Chem. C* 112:6891–99
67. Nagaoka S, Matsumoto T, Okada E, Mitsui M, Nakajima A. 2006. Room-temperature isolation of V(benzene)<sub>2</sub> sandwich clusters via soft-landing into *n*-alkanethiol self-assembled monolayers. *J. Phys. Chem. B* 110:16008–17
68. Nagaoka S, Okada E, Doi S, Mitsui M, Nakajima A. 2005. Trapping of V(benzene)<sub>2</sub> sandwich clusters in a *n*-alkanethiol self-assembled monolayer matrix. *Eur. Phys. J. D* 34:239–42
69. Shen JW, Evans C, Wade N, Cooks RG. 1999. Ion-ion collisions leading to formation of C–C bonds at surfaces: an interfacial Kolbe reaction. *J. Am. Chem. Soc.* 121:9762–63
70. Wang P, Laskin J. 2009. Surface modification using reactive landing of mass-selected ions. In *Ion Beams in Nanoscience and Technology*, ed. R Hellborg, HJ Whitlow, Y Zhang, pp. 37–65. London/New York: Springer
71. Wade N, Evans C, Jo SC, Cooks RG. 2002. Silylation of an OH-terminated self-assembled monolayer surface through low-energy collisions of ions: a novel route to synthesis and patterning of surfaces. *J. Mass Spectrom.* 37:591–602
72. Ada ET, Kornienko O, Hanley L. 1998. Chemical modification of polystyrene surfaces by low-energy polyatomic ion beams. *J. Phys. Chem. B* 102:3959–66
73. Wijesundara MJB, Hanley L, Ni B, Sinnott SB. 2000. Effects of unique ion chemistry on thin-film growth by plasma-surface interactions. *Proc. Natl. Acad. Sci. USA* 97:23–27

74. Palmer RE, Pratontep S, Boyen HG. 2003. Nanostructured surfaces from size-selected clusters. *Nat. Mater.* 2:443–48
75. Gao L, Lyn ME, Bergeron DE, Castleman AW. 2003. Met-Cars: mass deposition and preliminary structural study via TEM. *Int. J. Mass Spectrom.* 229:11–17
76. Löffler D, Jester SS, Weis P, Bottcher A, Kappes MM. 2006.  $C_n$  films ( $n = 50, 52, 54, 56$ , and  $58$ ) on graphite: cage size dependent electronic properties. *J. Chem. Phys.* 124:054705
77. Wysocki VH, Jones CM, Galhena AS, Blackwell AE. 2008. Surface-induced dissociation shows potential to be more informative than collision-induced dissociation for structural studies of large systems. *J. Am. Soc. Mass Spectrom.* 19:903–13
78. Grill V, Shen J, Evans C, Cooks RG. 2001. Collisions of ions with surfaces at chemically relevant energies: instrumentation and phenomena. *Rev. Sci. Instrum.* 72:3149–79
79. Laskin J, Futrell JH. 2003. Collisional activation of peptide ions in FT-ICR mass spectrometry. *Mass Spectrom. Rev.* 22:158–81
80. Laskin J, Futrell JH. 2005. Activation of large ions in FT-ICR mass spectrometry. *Mass Spectrom. Rev.* 24:135–67
81. Vekey K, Somogyi A, Wysocki VH. 1995. Internal energy-distribution of benzene molecular ions in surface-induced dissociation. *J. Mass Spectrom.* 30:212–17
82. Wysocki VH, Joyce KE, Jones CM, Beardsley RL. 2008. Surface-induced dissociation of small molecules, peptides, and non-covalent protein complexes. *J. Am. Soc. Mass Spectrom.* 19:190–208
83. Jacobs DC. 2002. Reactive collisions of hyperthermal energy molecular ions with solid surfaces. *Annu. Rev. Phys. Chem.* 53:379–407
84. Cooks RG, Ast T, Pradeep T, Wysocki V. 1994. Reactions of ions with organic surfaces. *Acc. Chem. Res.* 27:316–23
85. Gologan B, Wiseman JM, Cooks RG. 2006. Ion soft landing: instrumentation, phenomena, and applications. In *Principles of Mass Spectrometry Applied to Biomolecules*, ed. J Laskin, C Lifshitz, pp. 443–74. Hoboken: Wiley
86. Laskin J, Wang P, Hadjar O. 2010. Soft-landing of  $Co^{III}(\text{salen})^+$  and  $Mn^{III}(\text{salen})^+$  on self-assembled monolayer surfaces. *J. Phys. Chem. C* 114:5305–11
87. Shen JW, Yim YH, Feng BB, Grill V, Evans C, Cooks RG. 1999. Soft landing of ions onto self-assembled hydrocarbon and fluorocarbon monolayer surfaces. *Int. J. Mass Spectrom.* 183:423–35
88. Volny M, Sengupta A, Wilson CB, Swanson BD, Davis EJ, Turecek F. 2007. Surface-enhanced Raman spectroscopy of soft-landed polyatomic ions and molecules. *Anal. Chem.* 79:4543–51
89. Reimer U, Reineke U, Schneider-Mergener J. 2002. Peptide arrays: from macro to micro. *Curr. Opin. Biotechnol.* 13:315–20
90. Mrksich M, Whitesides GM. 1996. Using self-assembled monolayers to understand the interactions of man-made surfaces with proteins and cells. *Annu. Rev. Biophys. Biomol. Struct.* 25:55–78
91. Ratner BD, Bryant SJ. 2004. Biomaterials: where we have been and where we are going. *Annu. Rev. Biomed. Eng.* 6:41–75
92. Gurard-Levin ZA, Mrksich M. 2008. Combining self-assembled monolayers and mass spectrometry for applications in biochips. *Annu. Rev. Anal. Chem.* 1:767–800
93. Jonkheijm P, Weinrich D, Schroder H, Niemeyer CM, Waldmann H. 2008. Chemical strategies for generating protein biochips. *Angew. Chem. Int. Ed.* 47:9618–47
94. Niemeyer CM. 2010. Semisynthetic DNA-protein conjugates for biosensing and nanofabrication. *Angew. Chem. Int. Ed.* 49:1200–16
95. Love JC, Estroff LA, Kriebel JK, Nuzzo RG, Whitesides GM. 2005. Self-assembled monolayers of thiolates on metals as a form of nanotechnology. *Chem. Rev.* 105:1103–69
96. Wong LS, Khan F, Micklefield J. 2009. Selective covalent protein immobilization: strategies and applications. *Chem. Rev.* 109:4025–53
97. Hadjar O, Futrell JH, Laskin J. 2007. First observation of charge reduction and desorption kinetics of multiply protonated peptides soft landed onto self-assembled monolayer surfaces. *J. Phys. Chem. C* 111:18220–25

98. Wade N, Gologan B, Vincze A, Cooks RG, Sullivan DM, Bruening ML. 2002. Esterification and ether formation at a hydroxyl-terminated self-assembled monolayer surface using low-energy collisions of polyatomic cations. *Langmuir* 18:4799–808
99. Schreiber F, Gerstenberg MC, Dosch H, Scoles G. 2003. Melting point enhancement of a self-assembled monolayer induced by a van der Waals bound capping layer. *Langmuir* 19:10004–6
100. Hu QC, Wang P, Gassman PL, Laskin J. 2009. In situ studies of soft- and reactive landing of mass-selected ions using infrared reflection absorption spectroscopy. *Anal. Chem.* 81:7302–8
101. Mazzei F, Favero G, Frasconi M, Tata A, Tuccitto N, et al. 2008. Soft-landed protein voltammetry: a tool for redox protein characterization. *Anal. Chem.* 80:5937–44
102. Pepi F, Ricci A, Tata A, Favero G, Frasconi M, et al. 2007. Soft landed protein voltammetry. *Chem. Commun.* 2007:3494–96
103. Mazzei F, Favero G, Frasconi M, Tata A, Pepi F. 2009. Electron-transfer kinetics of microperoxidase-11 covalently immobilised onto the surface of multi-walled carbon nanotubes by reactive landing of mass-selected ions. *Chem. Eur. J.* 15:7359–67
104. Yasutomi S, Morita T, Kimura S. 2005. pH-controlled switching of photocurrent direction by self-assembled monolayer of helical peptides. *J. Am. Chem. Soc.* 127:14564–65
105. Davie EAC, Mennen SM, Xu YJ, Miller SJ. 2007. Asymmetric catalysis mediated by synthetic peptides. *Chem. Rev.* 107:5759–812
106. Hu QC, Wang P, Laskin J. 2010. Effect of the surface on the secondary structure of soft landed peptide ions. *Phys. Chem. Chem. Phys.* 12:12802–10
107. Mandal HS, Kraatz HB. 2007. Effect of the surface curvature on the secondary structure of peptides adsorbed on nanoparticles. *J. Am. Chem. Soc.* 129:6356–57
108. Capriotti LA, Beebe TP, Schneider JP. 2007. Hydroxyapatite surface-induced peptide folding. *J. Am. Chem. Soc.* 129:5281–87
109. Michael KE, Vernekar VN, Keselowsky BG, Meredith JC, Latour RA, Garcia AJ. 2003. Adsorption-induced conformational changes in fibronectin due to interactions with well-defined surface chemistries. *Langmuir* 19:8033–40
110. Sethuraman A, Belfort G. 2005. Protein structural perturbation and aggregation on homogeneous surfaces. *Biophys. J.* 88:1322–33
111. Rieu JP, Ronzon F, Roux B. 2002. Adsorption and aggregation of glycosylphosphatidyl inositol (GPI) anchored alkaline phosphatase on methylated glass surfaces studied by tapping mode atomic force microscopy. *Thin Solid Films* 406:241–49
112. Dubreil L, Vie V, Beauflis S, Marion D, Renault A. 2003. Aggregation of puroindoline in phospholipid monolayers spread at the air-liquid interface. *Biophys. J.* 85:2650–60
113. Marchin KL, Berrie CL. 2003. Conformational changes in the plasma protein fibrinogen upon adsorption to graphite and mica investigated by atomic force microscopy. *Langmuir* 19:9883–88
114. Ertl G. 2008. Reactions at surfaces: from atoms to complexity (Nobel lecture). *Angew. Chem. Int. Ed.* 47:3524–35
115. Somorjai GA, Li YM. 2010. Major successes of theory-and-experiment-combined studies in surface chemistry and heterogeneous catalysis. *Top. Catal.* 53:311–25
116. Xia Y, Xiong YJ, Lim B, Skrabalak SE. 2009. Shape-controlled synthesis of metal nanocrystals: simple chemistry meets complex physics? *Angew. Chem. Int. Ed.* 48:60–103
117. Castleman AW, Khanna SN. 2009. Clusters, superatoms, and building blocks of new materials. *J. Phys. Chem. C* 113:2664–75
118. Bernhardt TM. 2005. Gas-phase kinetics and catalytic reactions of small silver and gold clusters. *Int. J. Mass Spectrom.* 243:1–29
119. Rottgen MA, Abbet S, Judai K, Antonietti JM, Worz AS, et al. 2007. Cluster chemistry: size-dependent reactivity induced by reverse spill-over. *J. Am. Chem. Soc.* 129:9635–39
120. Landman U, Yoon B, Zhang C, Heiz U, Arenz M. 2007. Factors in gold nanocatalysis: oxidation of CO in the non-scalable size regime. *Top. Catal.* 44:145–58
121. Gilb S, Arenz M, Heiz U. 2006. The polymerization of acetylene on supported metal clusters. *Low Temp. Phys.* 32:1097–103

122. Worz AS, Judai K, Abbet S, Heiz U. 2003. Cluster size-dependent mechanisms of the CO + NO reaction on small Pd<sub>n</sub> (*n* ≤ 30) clusters on oxide surfaces. *J. Am. Chem. Soc.* 125:7964–70
123. Hagen J, Socaciu LD, Heiz U, Bernhardt TM, Woste L. 2003. Size dependent reaction kinetics of small gold clusters with carbon monoxide: influence of internal degrees of freedom and carbonyl complex stability. *Eur. Phys. J. D* 24:327–30
124. Heiz U, Vanolli F, Sanchez A, Schneider WD. 1998. Size-dependent molecular dissociation on mass-selected, supported metal clusters. *J. Am. Chem. Soc.* 120:9668–71
125. Yoon B, Hakkinen H, Landman U, Worz AS, Antonietti JM, et al. 2005. Charging effects on bonding and catalyzed oxidation of CO on Au<sub>8</sub> clusters on MgO. *Science* 307:403–7
126. Sanchez A, Abbet S, Heiz U, Schneider WD, Hakkinen H, et al. 1999. When gold is not noble: nanoscale gold catalysts. *J. Phys. Chem. A* 103:9573–78
127. Lei Y, Mehmood F, Lee S, Greeley J, Lee B, et al. 2010. Increased silver activity for direct propylene epoxidation via subnanometer size effects. *Science* 328:224–28
128. Lee S, Molina LM, Lopez MJ, Alonso JA, Hammer B, et al. 2009. Selective propene epoxidation on immobilized Au<sub>6–10</sub> clusters: the effect of hydrogen and water on activity and selectivity. *Angew. Chem. Int. Ed.* 48:1467–71
129. Guo BC, Wei S, Purnell J, Buzza S, Castleman AW. 1992. Metallo-carbohedrenes [M<sub>8</sub>C<sub>12</sub><sup>+</sup> (M = V, Zr, Hf, and Ti)]—a class of stable molecular cluster ions. *Science* 256:515–16
130. Goldby IM, Kuipers L, von Issendorff B, Palmer RE. 1996. Diffusion and aggregation of size-selected silver clusters on a graphite surface. *Appl. Phys. Lett.* 69:2819–21
131. Tainoff D, Bardotti L, Tournus F, Guiraud G, Boisson O, Melinon P. 2008. Self-organization of size-selected bare platinum nanoclusters: toward ultra-dense catalytic systems. *J. Phys. Chem. C* 112:6842–49
132. Kenny DJ, Palmer RE, Sanz-Navarro CF, Smith R. 2002. Implantation depth of size-selected silver clusters into graphite. *J. Phys. Condens. Matter* 14:L185–91
133. Xirouchaki C, Palmer RE. 2002. Pinning and implantation of size-selected metal clusters: a topical review. *Vacuum* 66:167–73
134. Leung C, Xirouchaki C, Berovic N, Palmer RE. 2004. Immobilization of protein molecules by size-selected metal clusters on surfaces. *Adv. Mater.* 16:223–26
135. Notestein JM, Katz A. 2006. Enhancing heterogeneous catalysis through cooperative hybrid organic-inorganic interfaces. *Chem. Eur. J.* 12:3954–65
136. Baker RT, Kobayashi S, Leitner W. 2006. Divide et impera—multiphase, green solvent and immobilization strategies for molecular catalysis. *Adv. Synth. Catal.* 348:1337–40
137. Coperet C, Chabanas M, Saint-Arroman RP, Basset JM. 2003. Homogeneous and heterogeneous catalysis: bridging the gap through surface organometallic chemistry. *Angew. Chem. Int. Ed.* 42:156–81
138. Tsuchida E, Oyaizu K. 2003. Oxovanadium(III)-V mononuclear complexes and their linear assemblies bearing tetradentate Schiff base ligands: structure and reactivity as multielectron redox catalysts. *Coord. Chem. Rev.* 237:213–28
139. Yamamoto K, Oyaizu K, Tsuchida E. 1996. Catalytic cycle of a divanadium complex with salen ligands in O<sub>2</sub> reduction: two-electron redox process of the dinuclear center [salen equals *N,N'*-ethylenebis(salicylideneamine)]. *J. Am. Chem. Soc.* 118:12665–72



# Contents

A Century of Progress in Molecular Mass Spectrometry <i>Fred W. McLafferty</i> .....	1
Modeling the Structure and Composition of Nanoparticles by Extended X-Ray Absorption Fine-Structure Spectroscopy <i>Anatoly I. Frenkel, Aaron Yevick, Chana Cooper, and Relja Vasic</i> .....	23
Adsorption Microcalorimetry: Recent Advances in Instrumentation and Application <i>Matthew C. Crowe and Charles T. Campbell</i> .....	41
Microfluidics Using Spatially Defined Arrays of Droplets in One, Two, and Three Dimensions <i>Rebecca R. Pompano, Weishan Liu, Wenbin Du, and Rustem F. Ismagilov</i> .....	59
Soft Landing of Complex Molecules on Surfaces <i>Grant E. Johnson, Qichi Hu, and Julia Laskin</i> .....	83
Metal Ion Sensors Based on DNazymes and Related DNA Molecules <i>Xiao-Bing Zhang, Rong-Mei Kong, and Yi Lu</i> .....	105
Shell-Isolated Nanoparticle-Enhanced Raman Spectroscopy: Expanding the Versatility of Surface-Enhanced Raman Scattering <i>Jason R. Anema, Jian-Feng Li, Zhi-Lin Yang, Bin Ren, and Zhong-Qun Tian</i> .....	129
High-Throughput Biosensors for Multiplexed Food-Borne Pathogen Detection <i>Andrew G. Gebring and Shu-I Tu</i> .....	151
Analytical Chemistry in Molecular Electronics <i>Adam Johan Berggren and Richard L. McCreery</i> .....	173
Monolithic Phases for Ion Chromatography <i>Anna Nordborg, Emily F. Hilder, and Paul R. Haddad</i> .....	197
Small-Volume Nuclear Magnetic Resonance Spectroscopy <i>Raluca M. Fratila and Aldrik H. Velders</i> .....	227



The Use of Magnetic Nanoparticles in Analytical Chemistry <i>Jacob S. Beveridge, Jason R. Stephens, and Mary Elizabeth Williams</i>	251
Controlling Mass Transport in Microfluidic Devices <i>Jason S. Kuo and Daniel T. Chiu</i>	275
Bioluminescence and Its Impact on Bioanalysis <i>Daniel Scott, Emre Dikici, Mark Ensor, and Sylvia Daunert</i>	297
Transport and Sensing in Nanofluidic Devices <i>Kaimeng Zhou, John M. Perry, and Stephen C. Jacobson</i>	321
Vibrational Spectroscopy of Biomembranes <i>Zachary D. Schultz and Ira W. Levin</i>	343
New Technologies for Glycomic Analysis: Toward a Systematic Understanding of the Glycome <i>John F. Rakus and Lara K. Mahal</i>	367
The Asphaltenes <i>Oliver C. Mullins</i>	393
Second-Order Nonlinear Optical Imaging of Chiral Crystals <i>David J. Kissick, Debbie Wanapun, and Garth J. Simpson</i>	419
Heparin Characterization: Challenges and Solutions <i>Christopher J. Jones, Szabolcs Beni, John F.K. Limtiaco, Derek J. Langeslay, and Cynthia K. Larive</i>	439

## Indexes

Cumulative Index of Contributing Authors, Volumes 1–4	467
Cumulative Index of Chapter Titles, Volumes 1–4	470

## Errata

An online log of corrections to the *Annual Review of Analytical Chemistry* articles may be found at <http://arjournals.annualreviews.org/errata/anchem>